

Effective and Efficient Dropout for Deep Convolutional Neural Networks

Shaofeng Cai[†], Jinyang Gao^{‡*}, Meihui Zhang[‡], Wei Wang[†], Gang Chen[§], Beng Chin Ooi[†]

[†]*National University of Singapore*
{shaofeng, wangwei, ooi bc}@comp.nus.edu.sg

[‡]*Beijing Institute of Technology*
meihui_zhang@bit.edu.cn

[‡]*Alibaba Group*
jinyang.gjy@alibaba-inc.com

[§]*Zhejiang University*
cg@zju.edu.cn

ABSTRACT

Machine-learning-based data-driven applications have become ubiquitous, e.g., health-care analysis and database system optimization. Big training data and large (deep) models are crucial for good performance. Dropout has been widely used as an efficient regularization technique to prevent large models from overfitting. However, many recent works show that dropout does not bring much performance improvement for deep convolutional neural networks (CNNs), a popular deep learning model for data-driven applications. In this paper, we formulate existing dropout methods for CNNs under the same analysis framework to investigate the failures. We attribute the failure to the conflicts between the dropout and the batch normalization operation after it. Consequently, we propose to change the order of the operations, which results in new building blocks of CNNs. Extensive experiments on benchmark datasets CIFAR, SVHN and ImageNet have been conducted to compare the existing building blocks and our new building blocks with different dropout methods. The results confirm the superiority of our proposed building blocks due to the regularization and implicit model ensemble effect of dropout. In particular, we improve over state-of-the-art CNNs with significantly better performance of 3.17%, 16.15%, 1.44%, 21.46% error rate on CIFAR-10, CIFAR-100, SVHN and ImageNet respectively.

1. INTRODUCTION

Recently, with big data and the proliferation of machine learning, especially deep learning, there is a surge of machine-learning-based data-driven [25] applications including deep-learning-based video stream analysis [16], health-care analysis [3] and database system optimization [32, 22]. Deep learning models are going larger and deeper to increase the capacity for the seek of higher performance (e.g., accuracy). For example, deep convolutional neural networks (CNNs) have led to a series of breakthroughs on a variety of tasks [19, 6, 12]. State-of-the-art CNNs typically comprise of hundreds of layers with millions of parameters [13, 36].

However, large complex models are prone to overfitting, which is a fundamental challenge of machine learning. To alleviate overfitting, many explicit and implicit regularization methods have been proposed, including early stopping, weight decay, data augmentation etc. Dropout [28, 9] is empirically more attractive among the existing methods due to its simplicity and efficiency. Standard dropout randomly

deactivates neurons in neural networks during the training process, which regularizes the networks by discouraging complex co-adaptation and meanwhile provides an economical way of an implicit model ensemble of an exponentially large number of all possible subnets with parameter typing.

Recent applications of dropout in convolutional neural networks[7, 37, 13] fail to obtain significant performance improvement. Dropout [28, 9] is initially introduced in fully connected layers [19] of neural networks. Recent CNN models replace the fully connected layers with a global average pooling layer [21]. Many CNNs have tried to apply dropout to convolution layers. For instance, WRN [37] applies a dropout layer between the convolution layers in each residual convolutional building block. Dropout used in these CNNs is still on the neuron level, which turns out to be less effective. For example, even negative effects are observed [8] when applying dropout in the identity mapping part of the residual block in ResNet [7]. The effect of dropout in CNNs is further diminished by the introduction of other regularization techniques such as data augmentation and batch normalization [15].

To better integrate dropout into CNNs, we revisit the existing dropout methods applied at different structural levels, namely neuron, channel, path and layer level. By analogy with standard dropout in the neuron level, we present a unified framework to analyze the four dropout methods. They are denoted as drop-neuron, drop-channel, drop-path and drop-layer for the neuron, channel, path and layer level dropout respectively. To appreciate the reason why existing dropout methods fail when they are applied to convolutional layers of CNNs, we investigate the interaction between dropout and other techniques involved in training CNNs, including data augmentation and batch normalization [15]. We attribute the failure of standard dropouts to the increase of variance from random deactivation of the basic components, e.g. neurons in drop-neuron and channels in drop-channel, which conflicts with the essence of the batch normalization layer following each convolutional layer.

We therefore propose to reorder the dropout and batch normalization in the convolutional building blocks to address this problem. A convolutional building block contains a sequence of layers, including dropout layer, convolution layer, batch normalization layer, etc. As validated in extensive experiments, they achieve better performance than existing building blocks. The strengths of our proposed general training mechanisms for deep CNNs are three-fold. First, the proposed dropout building blocks are generally applicable to existing CNN architectures. Second, all of

*Jinyang Gao's work was done while he was in National University of Singapore.

these dropouts are computationally lightweight and imposes a negligible increase in model complexity. Third, the introduction of different levels of dropouts to convolutional layers of CNNs, especially drop-channel, provides a more general and effective regularization for CNNs which achieves state-of-the-art performance in a wide range of tasks, e.g. CIFAR-10, CIFAR-100 and SVHN. To support these claims, extensive experiments are conducted on state-of-the-art CNNs. We adopt widely benchmarked datasets CIFAR-10, CIFAR-100, SVHN and ImageNet where significant improvement in terms of accuracy is observed even with the presence of extensive data augmentation and batch normalization. With our proposed convolutional building blocks, we achieve significant improvement over state-of-the-art CNNs by 3.17% on CIFAR-10, 16.15% on CIFAR-100, and 1.44% on SVHN.

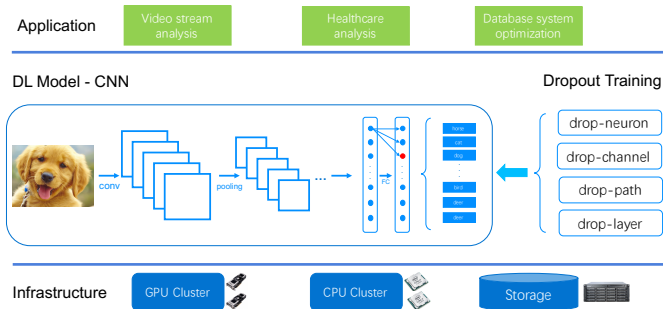


Figure 1: Architecture for dropout benchmark.

The main contributions of this paper are:

- We present a unified framework for analyzing dropout methods in CNNs. Specifically, we investigate the failure of two types of dropouts, which is mainly due to the incorrect placement of them in the convolutional building blocks.
- We propose new convolutional building blocks supporting dropout training mechanisms to better integrate dropouts, which are readily applicable to existing CNN architectures and harness the benefits of the regularization and model ensemble effect.
- Extensive experiments are conducted to compare different dropout methods and test the effectiveness of the proposed dropout convolutional building blocks as illustrated in Figure 1, with which we achieve significant improvement over state-of-the-art CNNs.

The remainder of the paper is organized as follows. Section 2 introduces the background, mainly focusing on the development of convolutional neural networks and dropout for deep neural networks. In Section 3, we formulate the convolutional transformation in a unified framework, based on which we propose training mechanisms of the four structural levels of dropouts incarnated in general convolutional building blocks for deep CNNs. Experimental evaluations of the effectiveness of our proposed convolutional building blocks are given in Section 4. Finally, we conclude the paper in Section 5.

2. BACKGROUND

2.1 Deep Convolutional Neural Networks

The development of convolutional neural networks (CNNs) in recent years mainly comes from the architecture engineering. One notable trend of latest state-of-the-art deep architectures is that they are going deeper and wider.

The trend of rapid growth of depth can be revealed from the winning models of the famous ILSVRC competition in recent years. AlexNet [19] wins the 2012 ILSVRC with an 8 layers CNN model. In 2014, VGG [26] and GoogLeNet [30] push the depth of CNNs to 19 and 22 respectively by stacking the basic convolutional building blocks, e.g. Inception module in GoogLeNet. One year later (2015), [7] propose a deep residual learning model ResNet. With the shortcut of identity mapping, ResNet enables the training of extremely deep CNNs over 1000 layers and wins the competition with an unprecedentedly 152 layers deep CNN.

Deeper CNNs undoubtedly provides larger representational capacity, while widening each layer can lead to better representation complementarily. [21] replaces the filter kernel of the convolutional transformation with multilayer perceptron. This Network In Network (NIN) structure allows complex and learnable interactions between input channels. Similar to NIN, CNNs such as Inception series [30, 29] and ResNeXt [36] explore group convolution [19], using multi-branches convolutional operation based on the idea of splitting, transforming and aggregating combination.

Besides the exploration of deeper and wider CNNs, new building blocks of CNNs have also been proposed, the stacking of which leads to state-of-the-art CNN architectures. For instance, the new convolutional layer NIN [21] and Inception modules [30] enable more complicated feature extractions with minimum additional parameters. Residual building blocks with identity mapping shortcuts [7, 8] make the training of deep CNNs possible. Dense blocks in DenseNet [13] are proposed to facilitate layer-wise feature reuse by forwarding input activation maps directly to output layers.

2.2 Dropout for Deep Neural Networks

Modern deep neural networks typically comprise up to hundreds of layers with millions of parameters. Regularization therefore, is of vital importance in these large models. Many regularization methods, mainly introduced during training, have been proposed to this end, including early stopping, weight decay, data augmentation, batch normalization [15] etc. Dropout [28, 9] stands out from these methods, which empirically proves to be an efficient and more importantly, effective regularization method.

To explain the effect of dropout, [34] shows that for generalized linear models, dropout performs a form of adaptive regularization. Theoretically, the dropout regularizer is first-order equivalent to an L_2 regularizer. [1] also shows that dropout provides immediately the magnitude of the regularization term which is adaptively scaled by the inputs and the variance of the dropout variables. [5, 17] instead formulate neural networks trained with dropout in the Bayesian inference framework, providing tools to model uncertainty with dropout training.

Apart from the regularization effect, dropout introduced to deep neural networks also harnesses the benefit of implicit model ensemble. Following this idea, many relevant techniques have subsequently been explored. Swapout generalizes dropout with a new stochastic training method, whose training process can be viewed as sampling from a rich archi-

ecture including dropout, stochastic depth [14] and residual architecture [7]. Unlike deactivating neurons in dropout, another work DropConnect [35] introduces randomness to connections and sets a randomly selected subset of weights within the network to zero during training. In DropIn [27], new layers are skipped at the start of the training, then increasingly including neurons from the new layers, which can be regarded as training a large collection of networks with varied architectures and extensive weight sharing.

Different levels of dropout have also been studied and introduced to deep convolutional neural networks. In [31], SpatialDropout shows that adding one additional layer with dropout applied to channels can achieve better performance in the specific task of object localization. In the path level, Drop-path proposed in FractalNet [20] randomly drops individual paths during training, preventing co-adaptation of parallel paths. In the layer level, Stochastic depth [14] randomly drops a subset of layers and forwards the information with identity mapping [7, 8] during training. This can be interpreted as layer-wise dropout, which achieves an ensemble of ResNets implicitly [33]. These dropout variants in convolutional neural networks apply dropout to basic units of CNNs, harnessing both the regularization and model ensemble benefits.

3. DROPOUT FOR CONVOLUTIONAL NEURAL NETWORKS

In this section, we first formulate the general transformation of convolutional neural networks in the viewpoint of split-transform-aggregate with the most fundamental components: neurons and channels respectively. Based on such formulation, we introduce general training mechanisms with drop-operations of different structural level deriving from dropout for deep CNNs. We also propose and examine various architectures of convolutional building blocks that are better in line with the dynamics of drop-operations introduced for deep CNNs.

3.1 The Linear and Convolution Transformations in Convolutional Neural Networks

Broadly speaking, the topology of neural networks, including vanilla neural networks, recurrent neural networks [2, 10] and convolutional neural networks [19, 7, 13], can be represented precisely by a set of connections among neurons, where the information flow from input neurons to output neurons is regulated by learnable weights coupled with each connection. Being the most basic unit of deep neural networks, each neuron aggregates information from its input neurons:

$$y_i = \sum_{j=1}^N w_{ij} x_j \quad (1)$$

where $\mathbf{x} = [x_1, x_2, \dots, x_N]$ is a N-dimension input vector and w_{ij} the weight coupled with the connection from input neuron x_j to the output neuron y_i . We omit output nonlinearity here for brevity. This neuron transformation is illustrated in Figure 2, which follows the strategy of split-transform-aggregate. The transformation can be interpreted as extracting features from all the input branches by first inner product transformation of input information with coupling weights and then aggregation over input dimensions.

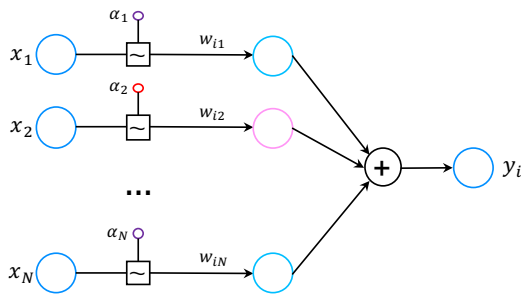


Figure 2: Simple neuron transformation for DNN

Besides neuron level representation, the transformation of convolutional neural networks can be formulated in a higher structural level with channels being the basic units. The most fundamental operation in CNNs comes from the convolutional layer which can be constructed to represent any given transformation $\mathcal{F}_{conv} : \mathbf{X} \rightarrow \mathbf{Y}$, where $\mathbf{X} \in \mathbb{R}^{C_{in} \times W_{in} \times H_{in}}$ is the input with C_{in} channels of size $W_{in} \times H_{in}$, $\mathbf{Y} \in \mathbb{R}^{C_{out} \times W_{out} \times H_{out}}$ the output likewise.

Denoting $\mathbf{X} = [\mathbf{x}_1, \mathbf{x}_2, \dots, \mathbf{x}_{C_{in}}]$ and $\mathbf{Y} = [\mathbf{y}_1, \mathbf{y}_2, \dots, \mathbf{y}_{C_{out}}]$ in vector representation of channels, the parameter set associated with each convolutional layer is a set of filter kernels $\mathbf{K} = [\mathbf{k}_1, \mathbf{k}_2, \dots, \mathbf{k}_{C_{out}}]$. The convolutional transformation on \mathbf{X} , therefore, can be succinctly represented as:

$$\mathbf{y}_i = \mathbf{k}_i * \mathbf{X} = \sum_{j=1}^{C_{in}} \mathbf{k}_i^j * \mathbf{x}_j \quad (2)$$

where $*$ denotes convolution, \mathbf{k}_i^j is a 2D spatial kernel associated with i_{th} output channel \mathbf{y}_i and convolves on j_{th} input channel \mathbf{x}_j . Each \mathbf{y}_i is typically followed by some output nonlinearity, which is omitted here for succinctness. We illustrate the channel level representation in Figure 3

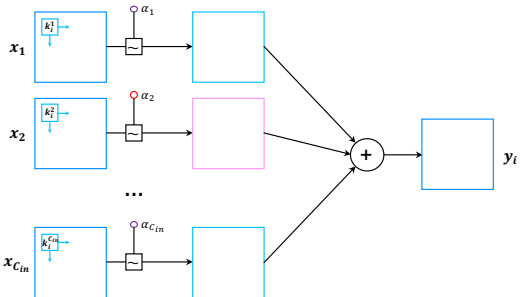


Figure 3: Channel transformation for CNN

We argue that the channel level representation is closer to the nature of convolutional transformation of CNNs. Structurally, CNNs consist of a stack of convolutional layers and for each convolutional layer, the transformation convolves over channels as is in Equation 2. Unlike dense layers such as fully connected layers where each connection between input and output neurons is coupled with one learnable weight, neurons in the same channel share one same filter kernel for each single output channel in CNNs. Such weight sharing strategy greatly reduces the number of parameters of CNNs and implicates that CNNs extract features in the

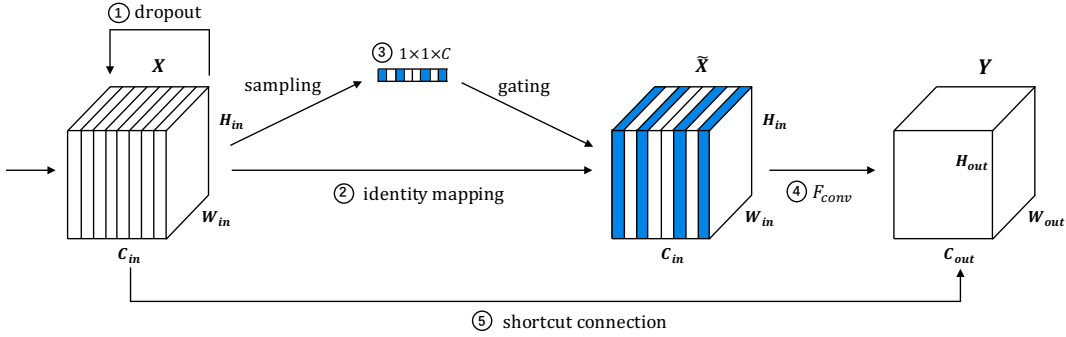


Figure 4: Illustration of various convolutional transformations. Dropout, or drop-neuron, gates input neurons in process 1; Drop-channel replaces identity mapping in process 2 with process 3, a random sampling and gating on channels; Drop-path is introduced to \mathcal{F}_{conv} in process 4 and Drop-layer to the shortcut connection in process 5.

channel level. This is corroborated by the visualization of convolutional kernels in AlexNet [19], filter kernels of the data-connected layer learn to identify orientations and colored blobs. In deconvnet visualization of ZFNet [39], output channels are also shown to detect certain kind of features, where increasing invariance and class discrimination is observed ascending the layers.

3.2 Drop-operations

In this subsection, we first recapitulate mainstream convolutional transformations of representative convolutional neural networks. To enhance the training of CNNs, four structural levels of drop-operations are introduced and analyzed. We then propose and examine general convolutional building blocks designed with built-in drop-operations and also general training mechanisms for deep CNNs.

3.2.1 Convolution Building Blocks

We illustrate mainstream convolutional transformation in Figure 4. Conventional convolutional transformation follows process 2 and 3, namely an identity mapping of \mathbf{X} and then a convolutional transformation \mathcal{F}_{conv} , which conforms to the formulation in Equation 2. It worth noting that group convolution [19] and depth-wise convolution [11] can also be represented under such formulation with customized constraints on the connection between channels.

One direction of mainstream exploration of convolutional transformation seeks to lengthen and/or widen the transformation here. For instance, NIN [21] lengthens \mathcal{F}_{conv} by following the traditional filter kernel with two layers of multi-layer perceptron transformation, which is structurally equivalent to appending it with two convolutional layers with 1×1 filter. Inception series [30, 29] widen \mathcal{F}_{conv} with multiple heterogeneous transformation branches. ResNeXt [36] follows similar strategy by duplicating it P times $\mathcal{F}_{conv}(\mathbf{X}) = \sum_{i=1}^P \mathcal{F}_{conv,i}(\mathbf{X})$, where the transformations are all of the same topology.

Another direction targets at the feature reuse by forwarding input channels information \mathbf{X} directly to output channels \mathbf{Y} , as is indicated in process 5. One commonly-adopted type of the feature reuse is a shortcut of identity mapping proposed in ResNet [7, 8], that is $\mathbf{Y} = \mathcal{F}_{conv}(\mathbf{X}) + \mathbf{X}$. The shortcut structure facilitates gradient flowing back and encourages residual learning. DenseNet [13] also proposes direct feature reuse by forwarding and appending

input channels \mathbf{X} directly to output channels \mathbf{Y} , specifically $\tilde{\mathbf{Y}} = [\mathbf{X}; \mathbf{Y}]$.

3.2.2 Drop-neuron - The Neuron Level Dropout

Dropout [28, 9] has been empirically shown to be an effective method of regularization and an economical way of model ensemble for deep neural networks. The standard dropout is applied to each single neuron during training, controlling the participation of each neuron x_j with a gating variable α_j for each forward pass:

$$y_i = \sum_{j=1}^N w_{ij}(\alpha_j \cdot x_j), \alpha_j \sim \text{Bernoulli}(1 - p_j) \quad (3)$$

Here \cdot denotes scalar multiplication and α_j is a Bernoulli random variable with probability p_j of being 0, $1 - p_j$ being 1. As is illustrated in Figure 2, the standard neuron level dropout, which we name it drop-neuron here to differentiate canonical dropout with other higher structural level of dropouts, introduces randomness to the training process which forces each neuron to learn more robust representations that are effective even with different random subsets of other neurons, thus improves generalization. More importantly, after training, rescaling each w_j with $1 - p_j$ [9, 28, 1], the resulting network then can be regarded as the ensemble network of many dropout subnets and therefore be used during inference time directly without dropout.

The neuron level dropout empirically demonstrates to be effective to improve generalization, especially for dense layers, as is illustrated in process 1 of Figure 4. For instance, dropout prevents overfitting significantly in the fully connected layers in the ILSVRC-2012 [4] winning CNN model AlexNet [19], and also recurrent layers in Neural Network Language Modeling models [23, 38]. However, recent state-of-the-art CNN models [7, 13, 12] no longer contains fully-connected layers, which are instead replaced by global average pooling [21]. Meanwhile, experiments in [7, 8, 37] find that dropout has very limited improvement when applied to convolutional layers. We conjecture that this is because structurally in CNNs, feature extractions are conducted channel-wisely during convolutional operation, thus neuron level dropout can hardly enjoy the ensemble benefits. Dropout, therefore, can only improve performance with the regularization effect, whose contribution is quite finite in CNNs with extensive data augmentation.

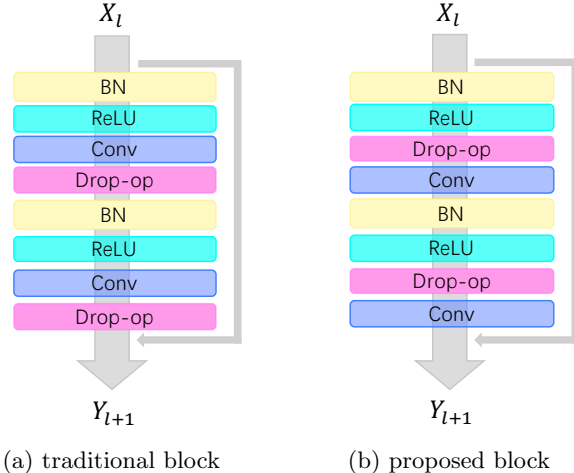


Figure 5: Example proposed convolutional building blocks with drop-operations, for both drop-channel and drop-neuron, in the Pre-activation convolutional transformation.

3.2.3 Drop-channel - The Channel Level Dropout

The channel level dropout, drop-channel, is inspired by the observation that there exists a close structural correspondence between channels in convolutional layer and neurons in vanilla neural networks, which is formulated formally in Equation 1, Equation 2 and illustrated in Figure 2, Figure 3. With similar derivation, drop-channel can be formally defined as:

$$\mathbf{y}_i = \mathbf{k}_i * \tilde{\mathbf{X}} = \sum_{j=1}^{C_{in}} \mathbf{k}_i^j * (\alpha_j \cdot \mathbf{x}_j) \quad (4)$$

where α_j is again a Bernoulli random variable with probability $1 - p_j$ of being 1 and is applied to the whole channel \mathbf{x}_j . In other words, α_j controls the presence of channel x_j during training. The drop-channel training is illustrated in Figure 4, where the identity mapping of process 2 is replaced by process 3, a random sampling of α_j followed by the corresponding gating. After training, a similar ensemble approximation strategy as is in drop-neuron can be achieved by rescaling each kernel weight \mathbf{k}_i^j on input channel \mathbf{x}_j with $1 - p_j$. The drop-channel approximation can also be efficiently achieved by rescaling those active activation maps \mathbf{x}_j of each channel with corresponding ratio $\frac{1}{1-p_j}$ in each forward pass during training, and the resulting network after training then can be directly used during inference time.

The idea of channel level dropout is first introduced in an object localization model named SpatialDropout [31]. However, experiments in [31] only show that SpatialDropout improve CNN models over a small dataset and the effectiveness and interaction of this channel level dropout technique in effect with other training techniques, e.g. data augmentation and batch normalization [15], are not properly examined. To exploit both regularization and ensemble effects to the largest extent, we investigate further in the complicated interaction between drop-channel and other training techniques widely used in state-of-the-art CNNs. Based on our observation and empirical evaluation, we propose gen-

eral convolutional building blocks for the training of deep CNNs.

$$\hat{\mathbf{x}} = \frac{\mathbf{x}_{in} - \mu}{\sqrt{\sigma^2 + \epsilon}}; \mathbf{x}_{out} = \gamma \hat{\mathbf{x}} + \beta \quad (5)$$

Each convolutional layer of state-of-the-art CNN models is typically coupled with a batch normalization layer (BN) [15] to normalize inputs batch-wisely, which stabilizes mean and variance of the input channels \mathbf{X} received by each output channel \mathbf{y}_i . Take traditional pre-activation convolutional layers [8, 13, 12] for example, the convolutional transformation follows a *BN - ReLU - Conv* pipeline, which is illustrated in Figure 5a. We argue that the drop-operation, including drop-neuron and drop-channel, is not incorporated into the convolutional transformation properly, which is either neglected by discarding this technique totally or used in an erroneous way. In the implementation of Equation 5, each BN layer normalizes inputs with the batch mean μ and variance σ and keeps records of running estimates of them which will be directly used after training.

However, drop-operation is traditionally introduced right after convolutional layer and before BN layer, which leads to violent fluctuation of the mean and variance of inputs received by BN layers, especially for drop-channel. We attribute the failure of the standard dropout to the incorrect placement of drop-operations and propose general convolutional building blocks with drop-operations incorporated right before each convolutional layer in Figure 5b, BOTH FOR drop-channel and drop-neuron. The introduction of drop-operations before convolutional operation, as is also demonstrated in the local reparameterization of the variational dropout [17], has lower gradient variance and generally leads to much faster convergence. Extensive experiments on various state-of-the-art CNNs validate the superiority of our proposed convolutional building blocks in Section 4.

3.2.4 Higher Level Dropout: Drop-path and Drop-layer

Path level (drop-path) and layer level (drop-layer) dropout are proposed in FractalNet [20] and ResNet with Stochastic Depth [14] respectively. Although these two higher level dropouts are effective in regularizing CNNs, they are highly dependent on CNN architectures.

Specifically, drop-path requires CNN contains multiple paths of \mathcal{F}_{conv} in process 4 and drop-layer demands shortcut connection of process 5 illustrated in Figure 4. Formally, drop-path can be formulated as:

$$\mathbf{Y} = \mathcal{F}_{conv}(\mathbf{X}) = \sum_{i=1}^P \alpha_i \cdot \mathcal{F}_{conv,i}(\mathbf{X}) \quad (6)$$

where α_i is the same Bernoulli gating variable and controls the participation of i_{th} path in the convolutional transformation with probability $1 - p_i$. In FractalNet, the original drop-path is applied to the fractal architecture, where paths are heterogeneous and deviate from conventional CNN architectures. To make drop-path more applicable, we reincarnate drop-path as general convolutional building blocks, mainly inspired by the bottleneck structure [7] and group convolution [19].

Typically in the convolutional building block, the number of input and output channels is the same: $C_{in} = C_{out} = C$.

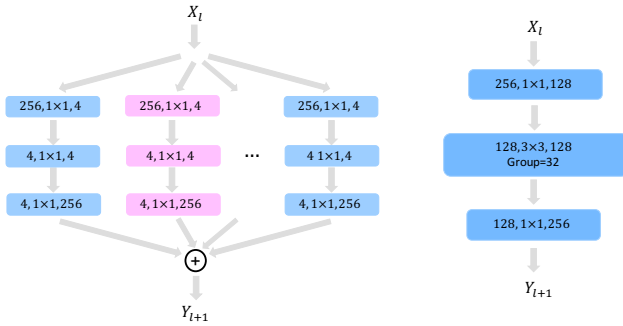


Figure 6: Convolutional building blocks supporting drop-path with bottleneck and group convolution.

We illustrate in Figure 6 a building blocks supporting drop-path for input \mathbf{X} and output \mathbf{Y} with $C = 256$ channels. The building block is resting on the parameter efficient bottleneck structure of one 3×3 convolution surrounded by dimensionality reducing and expanding with 1×1 convolution, namely $\text{conv}1 \times 1 - \text{conv}3 \times 3 - \text{conv}1 \times 1$. To support drop-path, we introduce group convolution to the inner 3×3 convolutional layer with P groups. Then structurally, the bottleneck building block contains P independent paths of homogeneous transformations, each of which first collapses C channels input into d channels by 1×1 convolution, then transforms by inner 3×3 convolution within each path and finally expand back to C channels altogether by 1×1 convolution. In the implementation, the transformation of this building block is equivalent to the original bottleneck with the introduction of group convolution to the inner 3×3 convolution, as is illustrated in the right panel of Figure 6. The total number of parameters contained in the convolutional building block is:

$$P \cdot C \cdot d \cdot 2 + P \cdot d^2 \cdot 3 \cdot 3 = P \cdot d \cdot (2 \cdot C + 9 \cdot d) \quad (7)$$

To find out the relationship between path number P , path channel width d and input/output channel number C , we follow the strategy of keeping the number of parameters roughly the same, meanwhile exploiting the benefits of drop-path further with the largest possible number of paths P . Since the original bottleneck parameter number is $C \cdot \frac{C}{4} \cdot 2 + (\frac{C}{4})^2 \cdot 3 \cdot 3 \approx C^2$ and with large P , $9 \cdot d \ll 2 \cdot C$, we therefore have the relationship that:

$$P \cdot d \approx \frac{C}{2}, \text{ s.t. } (9 \cdot d \ll 2 \cdot C) \wedge (P, d \in \mathbb{N}) \quad (8)$$

We further propose to choose P to be a power of 2 empirically, e.g. 16, 32, 64 and fixed P through out the network, and $d = \frac{C}{2 \cdot P}$ correspondingly. Take Figure 6 for example, channel width is 4 each group when there are 32 paths. During inference, the convolutional building blocks trained with drop-path also need to re-calibrate the activations of each path $\mathcal{F}_{\text{conv}_i}(\mathbf{X})$ by the expectation of the probability $1 - p_i$ that it participates in the forward pass.

For the layer level dropout, we also examine various architectures, e.g. randomly bypassing each convolutional layer with 1×1 shortcut transformation. However, we find out that drop-layer performs best when applied to the shortcut connection of identity mapping [8, 37], namely $\mathbf{Y} =$

$\mathcal{F}_{\text{conv}}(\mathbf{X}) + \mathbf{X}$, which is already analyzed extensively in ResNet with Stochastic Depth [14].

3.2.5 Comparison of Existing Dropout Methods

In the above subsections, we have already introduced and examined four different structural levels of dropout, namely drop-neuron, drop-channel, drop-path and drop-layer. Denoting the number of layers L , P paths each layer, channel width d each path with totally C channels each layer and input/output width/height W/H respectively, then the number of components for each stage before down-sampling in the convolutional neural network is summarized in Table 1.

Theoretically, the effectiveness of drop-operations comes from the regularization and ensemble effects [9, 34, 28], which is highly correlated with the number of basic components involved during dropout training. From Table 1, we note that the number of components decreases in orders of magnitude from neuron to layer level, which justifies the effectiveness decrease. However, there is one exception for drop-neuron, mainly because in CNNs, the neuron is not the basic unit participates in the convolutional transformation, therefore, the ensemble effect of it is less significant thus its effectiveness diminishes.

dropout level	neuron	channel	path	layer
granularity	N	C	P	L
components	$LPdWH$	LPd	LP	L
applicability	✓✓✓	✓✓✓	✓✓	✓
effectiveness	✓✓	✓✓✓	✓✓	✓

Table 1: Summary of various dropout levels for CNNs.

The applicability is another dimension when applying these drop-operations to CNNs. As we have already discussed along with the introduction of the four levels of dropout techniques, drop-neuron and drop-channel are readily applicable to existing CNNs with minor modification of placing the drop-op right before each convolutional transformation, and we have also proposed general convolutional building blocks in Section 3.2.4 which support drop-path regularization. Drop-layer is, however, highly dependent on the shortcut connection of process 5 in Figure 4 which is only applicable to CNNs with residual connections [7, 8, 37, 36].

We finally point out that these general dropout training mechanisms can be easily introduced to existing deep CNNs with the replacement of original convolutional transformation to our proposed convolutional building blocks support corresponding levels of dropout operations and share the only hyper-parameter dropout rate p among all the dropout components in the network for the desired regularization strength. Furthermore, these four levels of dropout operation ARE NOT mutually exclusive of each other. That is, they can co-exist in the same network whenever the CNN architecture allows for it, exploiting the benefits of dropout to the largest extent. It also worth noting that applying these drop-operations to CNNs introduces no additional model parameter, adds negligible computational cost for drop-neuron and drop-channel, and even reduces training time considerably for drop-path and drop-layer [14].

4. EXPERIMENTS

Group	Output Size	VGG-11	WRN-40-4	WRN-16-8	ResNeXt-29-P64-d4	DenseNet-L190-K40
conv1	32×32	[conv3×3, 64]×2	[conv3×3, 16]×1	[conv3×3, 16]×1	[conv3×3, 64]×1	[conv3×3, 80]×1
conv2	32×32	-	[Block, 16×4]×6	[Block, 16×8]×2	[B-Block, 256]×4	[D-Block, 80-1320]×31
conv3	16×16	[conv3×3, 256]×2	[Block, 32×4]×6	[Block, 32×8]×2	[B-Block, 512]×4	[D-Block, 660-1900]×31
conv4	8×8	[conv3×3, 256]×2	[Block, 64×4]×6	[Block, 64×8]×2	[B-Block, 1024]×4	[D-Block, 950-2190]×31
conv5	8×8	[conv3×3, 512]×4	-	-	-	-
avgPool	1×1	[avg8×8, 512]	[avg8×8, 256]	[avg8×8, 512]	[avg8×8, 1024]	[avg8×8, 2190]
Dataset	-	CIFAR	CIFAR	SVHN	CIFAR	CIFAR
Params	-	9.89M	8.95M	10.96M	8.85M	25.62M

Table 2: Detailed Architectures and configurations of representative convolutional neural networks for CIFAR and SVHN datasets. Building blocks are denoted as “[block, number of channels] × number of blocks”.

We evaluate the four levels of dropouts on representative state-of-the-art CNNs on widely compared benchmark datasets, including CIFAR, SVHN and ImageNet. In this section, we first introduce dataset details, CNN architectures and corresponding training details adopted. Secondly, we evaluate the effectiveness of convolutional building blocks with proposed drop-operations of drop-neuron and drop-channel, which is the foundation for the new state-of-the-art results on CIFAR and SVHN datasets. Then we compare drop-neuron, drop-channel, drop-path and drop-layer together with their combinations on representative CNN architectures, based on which we propose enhancement for existing best models on CIFAR and SVHN datasets and achieve a significant better results.

4.1 Dataset Details

The performance of dropout training mechanisms are evaluated on benchmark image classification datasets CIFAR[18], SVHN[24] and ImageNet[4]. Details of these datasets are given in this subsection.

4.1.1 CIFAR

The two CIFAR [18] datasets consist of 32×32 RGB scenery images. CIFAR-10 (C10) consists of images drawn from 10 classes and CIFAR-100 (C100) from 100 classes. The training and testing set for both datasets contain 50,000 and 10,000 images respectively. Following the standard data augmentation scheme [7, 14, 13], each image is first zero-padded with 4 pixels on each side, then randomly cropped to produce 32×32 images again, followed by a random horizontal flip. We denote the datasets with data augmentation by “+” behind the dataset names (e.g., C10+). For data preprocessing, we normalize each channel via standardization.

4.1.2 SVHN

The Street View House Numbers dataset [24] contains 32×32 colors digit images from Google Street View. The task is to correctly classify the central digit into one of the 10 digit classes. The training and testing sets respectively contain 73,257 and 26,032 images, and an additional training dataset contains 531,131 images that are relatively easier to classify. We adopt a common practice [14, 37, 13] by using all the training data without any data augmentation. Following [37, 13], we divide each pixel value by 255, scaling the input to range [0, 1].

4.1.3 ImageNet

The ILSVRC 2012 image classification dataset contains 1.2 million images for training and another 50,000 for validation from 1000 classes. We adopt the same data augmen-

tation scheme for training images following the convention[7, 37, 13], and apply a 224×224 center crop to images at test time. The results are reported on the validation set following common practice.

4.2 CNN Architecture Details

As summarized in Table 1, drop-neuron and drop-channel are applicable to general CNNs while the applicability of drop-path and drop-layer are dependent on the detailed CNN architectures. To evaluate the effectiveness of the four levels of dropout training mechanisms, we therefore adopt CNN architectures with representative convolutional transformation.

Specifically, we first evaluate and compare drop-neuron and drop-channel in our proposed convolutional building blocks illustrated in Figure 5b on VGG[26], whose convolutional layer is a plain 3×3 conv following process 2 and 4 of Figure 4. Then for drop-path of the new convolutional building block proposed in Section 3.2.4 and drop-layer, we test their effectiveness in comparison with drop-channel and drop-neuron on ResNeXt[36] with multiple paths and residual connection, Wide Residual Networks[37] (WRN) with wider convolutional layer and residual connection and DenseNet[13] with shortcut connection.

We denote these models adopted with WRN-depth-k, ResNeXt-depth-P-d and DenseNet-L-K, with k, P, d, L, K being widening factor[37], the number of paths, the channel width of each path[36], the number of layers (depth) and K the growth rate[13] respectively following the convention. The building blocks adopted for WRN, ResNeXt and DenseNet are basic block (Block) with two consecutive 3×3 conv, bottleneck block (B-Block) proposed in 3.2.4 and DenseNet bottleneck block (D-Block) [13] with dimensionality reduction of 1×1 conv and a following transformation of 3×3 conv. The detailed architectures and configurations of representative convolutional neural networks for CIFAR-10/100, SVHN and ImageNet datasets are provided in Table 2 and Table 3 respectively.

For CNNs with drop-neuron and drop-channel, each convolutional layer is replaced with our proposed convolutional building block in Section 3.2.4, where the drop-operations of drop-neuron and drop-channel are incorporated into the transformation right before the convolutional operation. While for CNNs with drop-path, we again replace each convolutional layer with the proposed general convolutional building block in Section 3.2.4 supporting drop-path with bottleneck and group convolution. The number of paths is the same for all the convolutional layers of the network and during training, each path is randomly being dropped following dropout dynamics.

Group	Output Size	VGG-16	Output Size	WRN-50-2	DenseNet-L169-K32
conv1	224×224	[conv3×3, 64]×2	112×112	conv7×7, stride 2	conv7×7, stride 2
pooling	112×112	2×2 max pool, stride 2	56×56	3×3 max pool, stride 2	3×3 max pool, stride 2
conv2	112×112	[conv3×3, 128]×2	56×56	[B-Block, 64×2]×6	[D-Block, 64-256]×6
pooling	56×56	2×2 max pool, stride 2	28×28	conv3×3, stride 2	Transition Layer
conv3	56×56	[conv3×3, 256]×2	28×28	[B-Block, 128×2]×3	[D-Block, 128-512]×12
pooling	28×28	2×2 max pool, stride 2	14×14	conv3×3, stride 2	Transition Layer
conv4	28×28	[conv3×3, 512]×2	14×14	[B-Block, 256×2]×3	[D-Block, 256-1792]×32
pooling	14×14	2×2 max pool, stride 2	7×7	conv3×3, stride 2	Transition Layer
conv5	14×14	[conv3×3, 512]×2	7×7	[B-Block, 512×2]×3	[D-Block, 896-1920]×32
pooling	7×7	2×2 max pool, stride 2	1×1	7×7, global avg-pool	7×7, global avg-pool
FC	1000	[512×7×7,4096,4096,1000]	1000	[1024,1000]	[1920,1000]
Params	-	138.4M	1	68.9M	14.1M

Table 3: Detailed Architectures and configurations of representative convolutional neural networks for ImageNet datasets. Building blocks are denoted as “[block, number of channels] × number of blocks”.

4.3 Training Details

In the experiments, we report the results in median over 5 runs. We train the networks with SGD + Nesterov momentum and cross-entropy loss, and we adopt weight initialization introduced by [6].

For CIFAR datasets, we train 300 epochs on VGG-11, ResNeXt-29-P64-d4, and DenseNet-L190-K40, 200 epochs on WRN-40-4. For SVHN, we train 160 epochs on WRN-16-8. The initial learning rate is set to 0.1, weight decay 0.0001, dampening 0, momentum 0.9 and mini-batch size 128 for CIFAR and SVHN datasets. The learning rate is divided by 10 at 50% and 75% of the total number of training epochs.

For ImageNet, we train 90 epochs on VGG-16, WRN-50-2, DenseNet-L169-K32 with a mini-batch size of 256. The initial learning rate is set 0.1, and is lowered by a factor of 10 after epoch 30 and epoch 60. We use a weight decay of 0.0001 and momentum 0.9 without dampening. Other training details follow their original settings.

4.4 Experimental Results

4.4.1 Building Blocks for Drop-neuron and Drop-channel

In this subsection, we validate the effectiveness of our proposed convolutional building blocks supporting drop-operation of drop-neuron and drop-channel. The CNN architectures adopted include VGG-11, WRN-40-4 and DenseNet-L100-K12, whose architectures follows the notation in Section 4.2 and Table 2. The results are reported on CIFAR-10 dataset.

Network	original	DN	DN+	DC	DC+
VGG	5.09	5.18	4.98 (+0.20)	4.78	4.67 (+0.11)
WRN	4.97	4.89	4.63 (+0.26)	4.60	4.31 (+0.29)
DenseNet	4.57	4.70	4.52 (+0.18)	4.56	4.32 (+0.24)

Table 4: Comparison of error rates (%) over Networks trained with drop-operations w/o our proposed convolutional building blocks on CIFAR-10.

The results are summarized in Table 4, where we report the results of networks trained without dropout (original), with original drop-neuron and drop-channel (DN and DC), and with our proposed drop-neuron and drop-channel (DN+ and DC+) respectively.

In Table 4, we can notice that our proposed convolutional building blocks consistently improve over their original blocks by a significant margin of around 0.20% accuracy. Another important finding is that comparing to their original results, networks trained with drop-neuron and drop-channel achieve significantly better performance, which demonstrates that dropout technique is effective in regularizing CNNs if applied properly. For instance, the introduction of drop-channel alone achieves absolute reduction of error rate 0.42%, 0.66% and 0.25% improvement of accuracy on VGG-11, WRN-40-4 and DenseNet-L100-K12 respectively.

4.4.2 Drop-operations w/o Data Augmentation

In this subsection, we test out drop-operations of drop-neuron and drop-channel for the training of CNNs. The results are reported on VGG-11 (see Table 2) trained with CIFAR-10 datasets, whose error rates and learning curves are illustrated in Figure 7 and Figure 8. We denote VGG networks trained without dropout, with drop-neuron and drop-channel as VGG-11, drop-neuron and drop-channel respectively, and the network trained with standard data augmentation is marked with a suffix +.

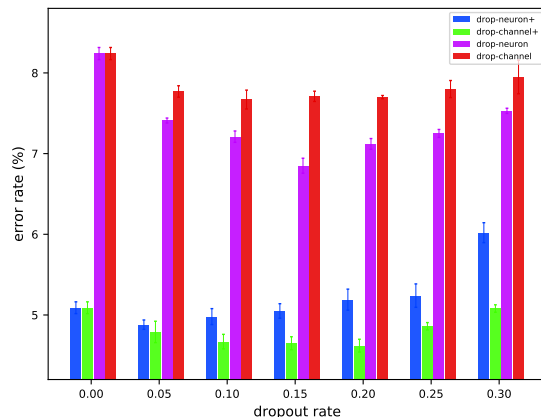


Figure 7: Error rate (%) of VGG-11 trained with drop-neuron and drop-channel w/o data augmentation.

We summarize the main results in Figure 7, where error rates and corresponding standard deviations are given with

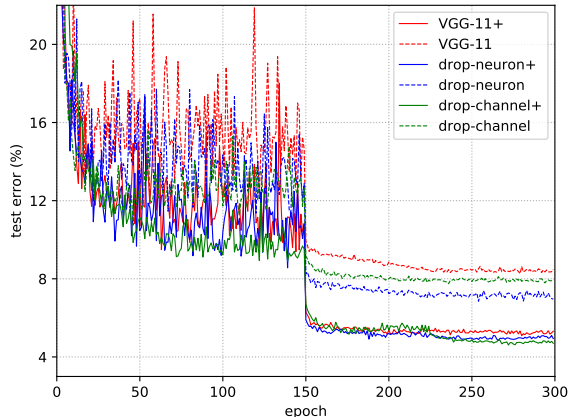


Figure 8: Learning curves of VGG-11 trained with no dropout, drop-neuron and drop-channel w/o data augmentation.

dropout rate in the granularity of 0.05. The results demonstrate that firstly, data augmentation is of vital importance for CNNs, without whose regularization effect, the performance deteriorates around 3%. Secondly, drop-neuron and drop-channel can improve over the performance both with and without data augmentation. Combined with data augmentation, drop-channel achieves the best result of 4.62% from 5.09%, 0.47% improvement, meanwhile without data augmentation, drop-neuron achieves the best accuracy of 6.85% from 8.24%, 1.39% improvement.

We further plot the learning curves of the networks trained with corresponding best settings in Figure 8. The learning curves corroborate the aforementioned findings and further demonstrate that drop-operations of drop-neuron and drop-channel are effective in regularizing CNNs. Furthermore, for state-of-the-art CNNs which are typically trained with extensive data augmentation, drop-channel is a powerful and general technique to improve the performance by a significant margin.

4.4.3 The effectiveness of Drop-path

In this subsection, we introduce drop-path to CNNs, specifically ResNeXt-29-64-4 from Table 2, and study the effect of this path level dropout in the training process alone and in combination with finer-grained drop-operations. We adopt convolutional building blocks supporting drop-path as is proposed in Section 3.2.4.

The results of ResNeXt trained with drop-neuron, drop-channel, drop-path and the combination of drop-path and drop-channel (drop-path-channel, results are reported with the same dropout rate from 0.05 to 0.15 for both drop-path and drop-channel) are summarized in Figure 9. We can notice that drop-neuron improves the performance mildly from 5.10% to 4.87%, and drop-channel outperforms drop-neuron with better error rate 4.72%. With our proposed drop-path building block, ResNeXt achieves even better result of 4.62%, which is 0.48% relative improvement over the network trained without any dropout.

More interestingly, as we have discussed in Section 3.2.5, path level dropout can be applied in combination with finer-

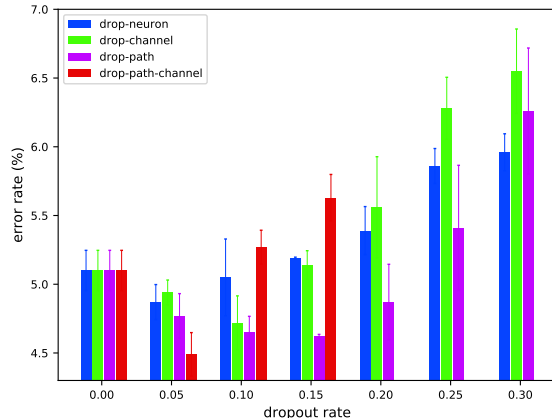


Figure 9: Error rate (%) of ResNeXt-29-64-4 trained with drop-neuron, drop-channel and drop-path.

grained drop-operations, namely drop-neuron and drop-channel. We therefore introduce the combination into ResNeXt and the results are even more encouraging. With the co-existence of drop-channel and drop-path, ResNeXt achieves the best result of 4.49 with dropout rate 0.05 for both levels of dropouts. This finding supports our assumption that combinations of different levels of dropouts could possibly further improve the performance of CNNs.

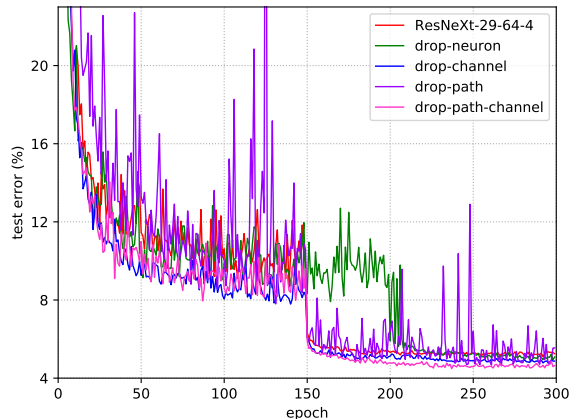


Figure 10: Learning curves of ResNeXt-29-64-4 trained with drop-neuron, drop-channel and drop-path.

To understand the impact of these dropouts on the training of CNNs, we plot the learning curves trained with dropouts of corresponding best dropout rates in Figure 10. We can notice that firstly, the network trained with each single dropout technique achieves notable better results than the one without by regularizing the learning process. Interestingly, the learning curves of networks trained with drop-path fluctuate drastically, though it achieves the best test accuracy than all other dropouts. However, when combined with drop-channel, this fluctuation is largely mitigated and more importantly, the combination yields the overall best result of

4.49% test error rate. We conjecture that this is mostly due to the fact that drop-path is a more radical regularization technique, where the whole path is dropped for those paths randomly being chosen, thus more susceptible to the removal of basic components from dropout. Therefore, a smaller dropout rate is preferable for higher level of dropouts, namely drop-path and drop-layer.

4.4.4 Drop-layer Revisiting

As we have discussed in Section 3.2.4 and Section 3.2.5, the effect of drop-layer is extensively studied in ResNet with Stochastic Depth [14] and [33]. To generalize drop-layer, we test out various design choices and find out that this layer level dropout is highly dependent on the residual connection of identity mapping introduced in [7, 8] which is later widely adopted in CNNs with residual connections [37, 36].

In this subsection, we focus mainly on the comparison of drop-layer with finer-grained levels of dropouts, namely drop-neuron and drop-channel, and the combination effect. We adopt WRN-40-4 (see Table 2) and test out different dropout techniques with dropout rate ranging from 0.0 to 0.40 in every 0.05. The main results are summarized in Figure 11 and Figure 12.

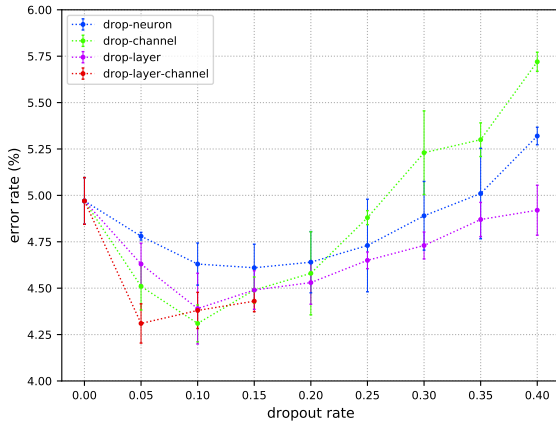


Figure 11: Error rate (%) of WRN-40-4 trained with drop-neuron, drop-channel and drop-layer.

In Figure 11, we find that firstly, all levels of dropouts achieve notable better results than the network trained without any dropout. In addition, drop-channel attains the best result of 0.66% relative improvement from test error rate 4.97% to 4.31%. When combined with drop-channel, drop-layer improves the performance slightly but the overall best result 4.31% is comparable to the effect of drop-channel alone.

To appreciate the dynamics involved, we further visualize learning curves of the error rates and losses in Figure 12. We can notice that the progression of the test error and the training loss corroborates the aforementioned claims. Another interesting finding is that the training loss of the network trained with drop-layer fluctuates drastically throughout the training process, although this is not reflected in the test error. We attribute the fluctuation to the radical reduction of basic components, specifically layers here, just like

drop-path. We therefore conclude that drop-channel is a favorable choice over drop-layer, which achieves better results with more stable training process.

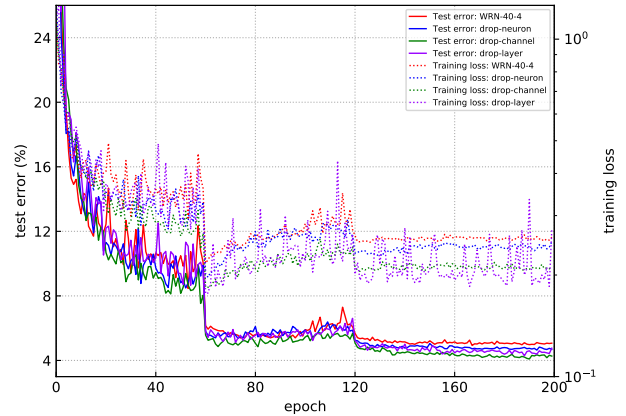


Figure 12: Learning curves and losses of WRN-40-4 trained with drop-neuron, drop-channel and drop-layer.

4.4.5 Dropouts: Better Results for State-of-the-art CNNs

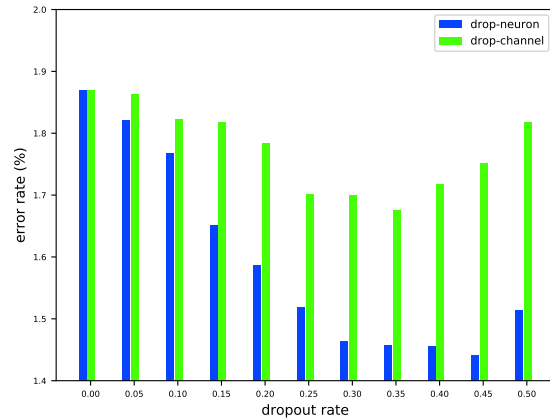


Figure 13: Error rate (%) of WRN-16-8 trained with drop-neuron and drop-channel on SVHN.

So far we have introduced the convolutional building blocks of different levels of dropouts for the enhancement of existing convolutional neural networks, meanwhile extensive experiments are conducted on these dropouts, namely drop-neuron, drop-channel, drop-path and drop-layer to validate their effectiveness.

With these dropout training mechanisms introduced to the toolbox, we then strive to improve the state-of-the-art model on benchmark datasets with better performance. The overall experimental results of CIFARs and SVHN datasets are summarized in Table 5. For SVHN, the current best reported result of 1.54% error rate is achieved by WRN-16-8 (Table 2) without data augmentation. We therefore

Model	Depth	Params	C10	C10+	C100	C100+	SVHN
VGG [26]	11	9.89M	8.24	5.09	23.58	32.08	-
↳with drop-neuron	11	9.89M	4.88	6.85	23.15	27.71	-
↳with drop-channel	11	9.89M	4.62	7.76	21.89	29.51	-
Wide ResNet [37]	40	8.95M	-	4.97	-	-	-
↳with drop-neuron	40	8.95M	-	4.61	-	-	-
↳with drop-channel	40	8.95M	-	4.31	-	-	-
↳with drop-layer	40	8.95M	-	4.39	-	-	-
Wide ResNet [37]	16	10.96M	-	-	-	-	1.54
↳with drop-neuron	16	10.96M	-	-	-	-	1.44
ResNeXt [36]	29	8.85M	-	5.10	-	-	-
↳with drop-neuron	29	8.85M	-	4.87	-	-	-
↳with drop-channel	29	8.85M	-	4.72	-	-	-
↳with drop-path	29	8.85M	-	4.62	-	-	-
DenseNet-BC (k=12) [13]	100	0.8M	5.92	4.51	24.15	22.27	1.76
↳with drop-channel	100	0.8M	5.59	4.24	23.73	20.75	1.65
DenseNet-BC (k=40) [13]	190	25.6M	-	3.46	-	17.18	-
↳with drop-neuron	190	25.6M	-	3.42	-	16.69	-
↳with drop-channel	190	25.6M	-	3.17	-	16.15	-

Table 5: Overall results in error rate (%) on CIFAR and SVHN datasets. A suffix + indicates standard data augmentation. We only list results discussed and compared in our Experiments Section 4 for succinctness. The overall best results are **blue**.

introduce our proposed drop-neuron and drop-channel convolutional building blocks to this network and the results are summarized in Figure 13 and Figure 14.

The results in Figure 13 corroborate that drop-neuron is more effective in regularizing the network trained without data augmentation. Replacing conventional convolutional layers with our drop-neuron convolutional building blocks in WRN-16-8, we achieve a better error rate of 1.44% on SVHN over the original state-of-the-art model. Figure 14 further shows that our proposed drop-neuron can effectively regularize the training process with significant lower training loss and also higher accuracy. Without dropout regularization, the training stagnates quickly and even deteriorate where the training loss and test error surge before the first learning rate drop. While with dropouts, the training is more stable and the network continues improving with higher accuracy.

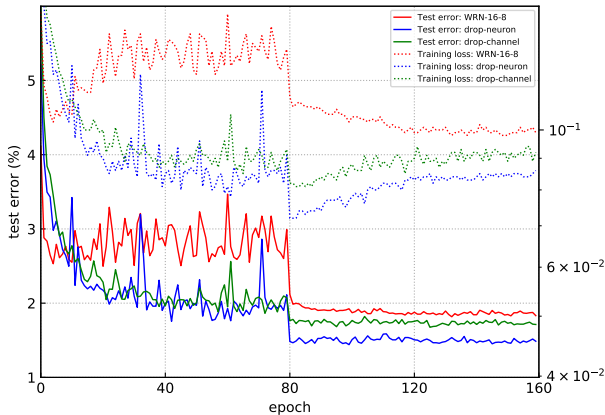


Figure 14: Learning curves and losses of WRN-16-8 trained with drop-neuron, drop-channel on SVHN.

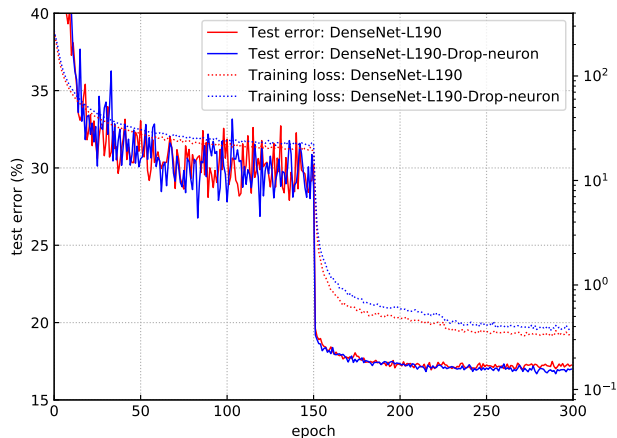
For CIFAR datasets, DenseNet-L190-K40 2 is the state-of-the-art model obtaining 4.36% and 17.18% error rates on CIFAR-10 and CIFAR-100 respectively. We apply drop-neuron and drop-channel convolutional building blocks in replacement of convolutional layers in the model and with dropout rate 0.1, significantly better results are achieved with 3.17% and 16.15% error rates, 0.29% and 1.03% relative improvement respectively.

Model	Depth	Params	ImageNet
VGG-16 [26]	16	138.4M	27.66
↳+drop-channel	16	138.4M	27.38
WRN-50-2 [37]	50	68.9M	21.90
↳+drop-layer+channel	50	68.9M	21.46
DenseNet-L169-K32 [13]	169	14.1M	23.60
↳+drop-path+channel	169	14.1M	23.17

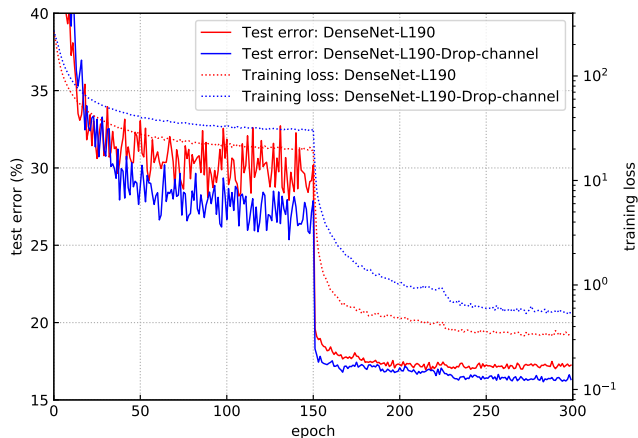
Table 6: Comparison of Top-1 (single model and single crop) error rates on ImageNet classification dataset.

The overall experimental results on ImageNet dataset are summarized in Table 6. Three representative CNN architectures are adopted for this large dataset, specifically VGG-16 [26] with plain convolutional operation, WRN-50-2 [37] with residual connection and DenseNet-L169-K32 [13] with dense connection between layers. For this large image classification dataset, we test the combination of drop-layer and drop-channel for WRN-50-2, meanwhile also the combination of drop-path and drop-channel for DenseNet-L169-K32.

For the plain CNN VGG-16, we obtain 0.28% accuracy improvement with drop-channel. For WRN-50-2, we observe larger improvement of 0.44% with the introduction of the combination of drop-layer and drop-channel. Lastly, with drop-path and drop-channel mechanisms introduced, DenseNet-L169-K32 achieves 0.43% error rate drop. The results of the three architectures on ImageNet further corroborate that the dropout training mechanisms, the application of the four levels of dropouts alone or their combination, can significantly improve the performance if adopted



(a) CIFAR-100 w/o drop-neuron



(b) CIFAR-100 w/o drop-channel

Figure 15: Test error and training loss curves for DenseNet-L190-K40 w/o drop-neuron and drop-channel. The two corresponding dropout rates are both set to 0.1, leading to 16.76% and 16.15% test error rate respectively on CIFAR-100+. Test error 17.18% is obtained without any dropout during training.

properly. The improvement demonstrates that our proposed dropout convolutional building blocks are also beneficial for large image classification dataset.

To illustrate the difference between the regularization effect of drop-neuron and drop-channel, we plot training curves of the 190 layer DenseNet on CIFAR-100+ with these two dropouts in Figure 15. Left panel indicates that the regularization effect of drop-neuron training is rather limited, which is mainly because channels instead of neurons are the most basic components involved in the convolutional transformation. Compared to drop-neuron, however, drop-channel regularizes the model effectively thus achieves significantly better performance. With drop-channel, the test error decreases faster and the training is more stable, especially before the first learning rate drop at epoch 150. Furthermore, DenseNet regularized by drop-channel learns with higher training loss yet much lower test error, indicating that drop-channel prevents overfitting effectively.

5. CONCLUSION

In this paper, we examine the four structural levels of dropout training mechanisms in a unified convolutional transformation framework, including drop-neuron, drop-channel, drop-path and drop-layer. We attribute the failure of standard dropout to the incorrect placement within the convolutional layer, which causes great training instability. Through detailed discussion and analysis, we propose general convolutional building blocks supporting different structural levels

of dropouts which are better in line with the convolutional transformation.

Extensive analysis and experiments demonstrate that firstly, all four levels of dropouts are effective in improving the performance of deep convolutional neural networks by a significant margin. Secondly, the applicability of them varies. Specifically, drop-neuron and drop-channel are widely applicable to existing CNNs while drop-path and drop-layer are highly dependent on the network architecture. Moreover, drop-neuron and drop-channel can be applied in combination with higher levels of dropouts, which can further stabilize the training process. Thirdly, in terms of effectiveness, drop-channel stands out from all other levels of dropouts. This results from the nature of the convolutional operation in CNNs, where the channel instead of other structural levels is the most fundamental transformation component. Therefore, drop-channel can harness the benefits of regularization and also model ensemble to the largest extent. On the other hand though, drop-neuron outperforms drop-channel in the network trained without data augmentation, as is shown in Section 4.4.2.

With our proposed convolutional building blocks specially designed for dropout training mechanisms, we achieve significant improvement over state-of-the-art CNNs on CIFAR-10/100, SVHN and ImageNet datasets. Given the generality and flexibility, these dropout training mechanisms would be useful for improving the performance for a wide range of deep CNNs.

6. REFERENCES

- [1] P. Baldi and P. J. Sadowski. Understanding dropout. In *Advances in Neural Information Processing Systems*, pages 2814–2822, 2013.
- [2] K. Cho, B. Van Merriënboer, D. Bahdanau, and Y. Bengio. On the properties of neural machine translation: Encoder-decoder approaches. *arXiv preprint arXiv:1409.1259*, 2014.
- [3] J. Dai, M. Zhang, G. Chen, J. Fan, K. Y. Ngiam, and B. C. Ooi. Fine-grained concept linking using neural networks in healthcare. In *Proceedings of the 2018 International Conference on Management of Data*, pages 51–66. ACM, 2018.
- [4] J. Deng, W. Dong, R. Socher, L.-J. Li, K. Li, and L. Fei-Fei. Imagenet: A large-scale hierarchical image database. In *Computer Vision and Pattern Recognition, 2009. CVPR 2009. IEEE Conference on*, pages 248–255. Ieee, 2009.
- [5] Y. Gal and Z. Ghahramani. Dropout as a bayesian approximation: Representing model uncertainty in deep learning. In *international conference on machine learning*, pages 1050–1059, 2016.
- [6] K. He, X. Zhang, S. Ren, and J. Sun. Delving deep into rectifiers: Surpassing human-level performance on imagenet classification. In *Proceedings of the IEEE international conference on computer vision*, pages 1026–1034, 2015.
- [7] K. He, X. Zhang, S. Ren, and J. Sun. Deep residual learning for image recognition. In *Proceedings of the IEEE conference on computer vision and pattern recognition*, pages 770–778, 2016.
- [8] K. He, X. Zhang, S. Ren, and J. Sun. Identity mappings in deep residual networks. In *European Conference on Computer Vision*, pages 630–645. Springer, 2016.
- [9] G. E. Hinton, N. Srivastava, A. Krizhevsky, I. Sutskever, and R. R. Salakhutdinov. Improving neural networks by preventing co-adaptation of feature detectors. *arXiv preprint arXiv:1207.0580*, 2012.
- [10] S. Hochreiter and J. Schmidhuber. Long short-term memory. *Neural computation*, 9(8):1735–1780, 1997.
- [11] A. G. Howard, M. Zhu, B. Chen, B. Kalenichenko, W. Wang, T. Weyand, M. Andreetto, and H. Adam. Mobilenets: Efficient convolutional neural networks for mobile vision applications. *arXiv preprint arXiv:1704.04861*, 2017.
- [12] J. Hu, L. Shen, and G. Sun. Squeeze-and-excitation networks. *arXiv preprint arXiv:1709.01507*, 2017.
- [13] G. Huang, Z. Liu, K. Q. Weinberger, and L. van der Maaten. Densely connected convolutional networks. *arXiv preprint arXiv:1608.06993*, 2016.
- [14] G. Huang, Y. Sun, Z. Liu, D. Sedra, and K. Q. Weinberger. Deep networks with stochastic depth. In *European Conference on Computer Vision*, pages 646–661. Springer, 2016.
- [15] S. Ioffe and C. Szegedy. Batch normalization: Accelerating deep network training by reducing internal covariate shift. In *International Conference on Machine Learning*, pages 448–456, 2015.
- [16] D. Kang, J. Emmons, F. Abuzaid, P. Bailis, and M. Zaharia. Noscope: Optimizing neural network queries over video at scale. *PVLDB*, 10(11):1586–1597, Aug. 2017.
- [17] D. P. Kingma, T. Salimans, and M. Welling. Variational dropout and the local reparameterization trick. In *Advances in Neural Information Processing Systems*, pages 2575–2583, 2015.
- [18] A. Krizhevsky and G. Hinton. Learning multiple layers of features from tiny images. *Tech Report*, 2009.
- [19] A. Krizhevsky, I. Sutskever, and G. E. Hinton. Imagenet classification with deep convolutional neural networks. In *Advances in neural information processing systems*, pages 1097–1105, 2012.
- [20] G. Larsson, M. Maire, and G. Shakhnarovich. Fractalnet: Ultra-deep neural networks without residuals. *arXiv preprint arXiv:1605.07648*, 2016.
- [21] M. Lin, Q. Chen, and S. Yan. Network in network. *arXiv preprint arXiv:1312.4400*, 2013.
- [22] L. Ma, D. Van Aken, A. Hefny, G. Mezerhane, A. Pavlo, and G. J. Gordon. Query-based workload forecasting for self-driving database management systems. In *Proceedings of the 2018 International Conference on Management of Data*, pages 631–645. ACM, 2018.
- [23] T. Mikolov, M. Karafiát, L. Burget, J. Černocký, and S. Khudanpur. Recurrent neural network based language model. In *Eleventh Annual Conference of the International Speech Communication Association*, 2010.
- [24] Y. Netzer, T. Wang, A. Coates, A. Bissacco, B. Wu, and A. Y. Ng. Reading digits in natural images with unsupervised feature learning. In *NIPS workshop on deep learning and unsupervised feature learning*, volume 2011, page 5, 2011.
- [25] C. Ré, D. Agrawal, M. Balazinska, M. Cafarella, M. Jordan, T. Kraska, and R. Ramakrishnan. Machine learning and databases: The sound of things to come or a cacophony of hype? In *Proceedings of the 2015 ACM SIGMOD International Conference on Management of Data*, pages 283–284. ACM, 2015.
- [26] K. Simonyan and A. Zisserman. Very deep convolutional networks for large-scale image recognition. *arXiv preprint arXiv:1409.1556*, 2014.
- [27] L. N. Smith, E. M. Hand, and T. Doster. Gradual dropin of layers to train very deep neural networks. In *Proceedings of the IEEE Conference on Computer Vision and Pattern Recognition*, pages 4763–4771, 2016.
- [28] N. Srivastava, G. E. Hinton, A. Krizhevsky, I. Sutskever, and R. Salakhutdinov. Dropout: a simple way to prevent neural networks from overfitting. *Journal of machine learning research*, 15(1):1929–1958, 2014.
- [29] C. Szegedy, S. Ioffe, V. Vanhoucke, and A. A. Alemi. Inception-v4, inception-resnet and the impact of residual connections on learning. In *AAAI*, pages 4278–4284, 2017.
- [30] C. Szegedy, W. Liu, Y. Jia, P. Sermanet, S. Reed, D. Anguelov, D. Erhan, V. Vanhoucke, and A. Rabinovich. Going deeper with convolutions. In *Proceedings of the IEEE conference on computer vision and pattern recognition*, pages 1–9, 2015.
- [31] J. Tompson, R. Goroshin, A. Jain, Y. LeCun, and C. Bregler. Efficient object localization using

- convolutional networks. In *Proceedings of the IEEE Conference on Computer Vision and Pattern Recognition*, pages 648–656, 2015.
- [32] D. Van Aken, A. Pavlo, G. J. Gordon, and B. Zhang. Automatic database management system tuning through large-scale machine learning. In *Proceedings of the 2017 ACM International Conference on Management of Data*, pages 1009–1024. ACM, 2017.
- [33] A. Veit, M. J. Wilber, and S. Belongie. Residual networks behave like ensembles of relatively shallow networks. In *Advances in Neural Information Processing Systems*, pages 550–558, 2016.
- [34] S. Wager, S. Wang, and P. S. Liang. Dropout training as adaptive regularization. In *Advances in neural information processing systems*, pages 351–359, 2013.
- [35] L. Wan, M. Zeiler, S. Zhang, Y. Le Cun, and R. Fergus. Regularization of neural networks using dropconnect. In *International Conference on Machine Learning*, pages 1058–1066, 2013.
- [36] S. Xie, R. Girshick, P. Dollár, Z. Tu, and K. He. Aggregated residual transformations for deep neural networks. In *2017 IEEE Conference on Computer Vision and Pattern Recognition (CVPR)*, pages 5987–5995. IEEE, 2017.
- [37] S. Zagoruyko and N. Komodakis. Wide residual networks. *arXiv preprint arXiv:1605.07146*, 2016.
- [38] W. Zaremba, I. Sutskever, and O. Vinyals. Recurrent neural network regularization. *arXiv preprint arXiv:1409.2329*, 2014.
- [39] M. D. Zeiler and R. Fergus. Visualizing and understanding convolutional networks. In *European conference on computer vision*, pages 818–833. Springer, 2014.